Journal of Atmospheric and Solar-Terrestrial Physics 71 (2009) 49–60

Contents lists available at ScienceDirect

Journal of Atmospheric and Solar-Terrestrial Physics

journal homepage: www.elsevier.com/locate/jastp

The main ionospheric trough in the East Asian region: Observation and modeling

O.M. Pirog *, N.M. Polekh, E.B. Romanova, A.V. Tashchilin, G.A. Zherebtsov

Institute of Solar-Terrestrial Physics, Irkutsk, Russian Academy of Sciences, Irkutsk, Russia

A R T I C L E I N F O

Article history:
Received 16 January 2008
Accepted 20 October 2008
Available online 31 October 2008

Keywords:
Ionospheric storm
Main ionospheric trough
Critical frequency
Drift
Numerical model and explanation

A B S T R A C T

Research results concerning the main ionospheric trough (MIT) in the afternoon sector are present. Data are used from the meridional chain of stations located in the East Asian region. The analysis of ionospheric storms with different intensities reveals that the depletion in the F2 layer ionization in the afternoon/evening sector can be observed in the subauroral latitudes in the storm recovery phase predominantly during equinoxes and is associated with the formation of the MIT equatorward wall. Model calculations of the evening trough show that its location coincides with the belt of westward drift in the geomagnetic latitudes 55–65° at 13–17 MLT. Hence the simulated results support the assumption that the narrow and deep trough in the afternoon sector is formed by the westward drift with high velocities (~700 m/s). the drift transports the low-density plasma from the night side. The eastward drift with high velocities (~1000–1200 m/s) transports the low-density plasma from the night to morning side forming a trough in the morning sector.

© 2008 Elsevier Ltd. All rights reserved.

1. Introduction

The space-temporal distribution of electron concentration in the high-latitude ionosphere is mainly determined by magnetospheric processes. In parallel with the solar illumination, there is an additional source of ionization in these latitudes: the precipitation of energetic particle fluxes. Satellite and ground-based observations allow the determination of the large-scale structure of the high-latitude ionosphere, whose elements are consistent with the structure of the magnetosphere (Buonsanto, 1999; Collis and Haggstrom, 1988; Evans et al., 1983a; Rodger et al., 1992). the high-latitude ionosphere can be studied and simulated only in terms of its large-scale structure. Of great interest is the main ionospheric trough (MIT) as a natural boundary between the middle and subauroral ionospheres. The ionospheric irregularities in the E and F regions and deep ionization gradients in the F2 layer at the polar MIT wall result from the combined action of auroral fluxes and electric fields in the auroral ionization zone (Benkova et al., 1980; Tsunoda, 1988). The MIT displacement to the equator during a geomagnetic storm causes typical subauroral phenomena observed in the middle latitudes (Kurkin et al., 2006).

A depleted region of the F2 layer ionization in the afternoon/evening sector has been observed for many years (Lockwood, 1980; Benkova et al., 1980; Besprozvannaya et al., 1986; Evans et al., 1983b; Holt et al., 1984; Whalen, 1987, 1989; Vo and Foster, 2001; Prölss et al., 1991; Prölss, 2007). In these papers, this region is termed daytime, midday, mid-latitude, and subauroral troughs.

Using data from the dense network of ground-based ionospheric stations, Whalen (1987, 1989) showed that the daytime trough can be observed as a characteristic “bite-out” in the local-time distribution of the ionospheric density (foF2). The foF2 can decrease by more than a factor of 2. This corresponds to the deep equatorial wall of the afternoon trough. This bite-out represents the leading

* Corresponding author.
E-mail address: pir@iszf.irk.ru (O.M. Pirog).

1364-6826/$ - see front matter © 2008 Elsevier Ltd. All rights reserved.
doi:10.1016/j.jastp.2008.10.010

edge of the daytime trough (LEDT). It was also designated as "fall of the foF2" (Benkova et al., 1980; Besprozvannaya et al., 1986).

The most likely explanation for the steep fall of electron density in the F layer maximum in the afternoon is the westward convection of plasma caused by the intense electric field. Satellite measurements show that intense poleward electric fields (~250 mV/m) can be observed on the equatorial wall of the auroral zone during geomagnetic storms (Rich et al., 1980). These fields are responsible for the westward drifts with velocities higher than 500 m/s (Holt et al., 1984; Foster, 1993). The high velocities result in deepening of the mid-latitude trough and its extension to the day sector. Subauroral ion drifts (SAID) are associated with disturbed conditions and specifically with a substorm recovery phase (Galperin et al., 1986; Anderson et al., 1993).

The discrepancy between geographic and geomagnetic coordinate systems leads to the longitudinal dependence in the high-latitude ionosphere structure (Afonin et al., 1995; Deminov and Karpachev, 1986a, b; Prölss, 2007). Longitudinal variations in the trough morphology have also been identified by ionosonde measurements (Whalen, 1987). The most distinctive difference between the geographic and geomagnetic latitudes is in the East Asian longitude sector. Thus, the subauroral trough, specifically its equatorward wall, forms on the background of the lower electron concentration in this region (Besprozvannaya et al., 1986; Zherebtsov et al., 1993; Afraimovich et al., 2005).

The purpose of this paper is to examine some peculiarities of the suburoral trough in the afternoon/evening sector in the East Asian region. In our analysis, we use data from the meridional chain of ionospheric stations, located in Eastern Siberia and China. Geomagnetic indices Dst, Kp, and AE from http://swdcwww.kugi.kyoto-u.ac.jp/wdc/Sec3.html are applied to estimate the geomagnetic situation.

Table 1
List of ionospheric stations.

Stations	Symbol	Geographic		Geomagnetic		*L*
		Latitude	Longitude	Latitude	Longitude	
Norilsk	NO	69.20	88.26	58.71	165.7	5.0
Zhigansk	ZH	66.3	123.4	55.2	190.0	4.1
Yakutsk	YA	62.0	129.6	51.0	194.1	3.1
Magadan	MG	60.12	151.0	50.75	210.8	2.7
Irkutsk	IR	52.5	104.0	41.1	174.8	2.1
Manzhouli	ML	49.6	117.5	38.4	186.5	1.9
Khabarovsk	KB	48.5	135.1	38.1	201.3	1.9
Beijing	BP	40.0	116.0	28.7	188	1.4

2. Experimental data

We study storms with different intensities observed from 2000 to 2007. Table 1 presents the list of ionospheric stations, whose data are used in this study. Table 2 presents the list of storms during which the foF2 fall is observed. The date, Dst_{min}, UT of Dst_{min}, the number of marked events, and the storm phase are indicated.

Note that LT is defined as LT = UT+Δt, where Δt varies from about 6 to 8 h depending on the longitude of a station (see Table 1).

According to Table 2, the foF2 fall can be observed in the East Asian sector predominantly in equinox or between equinox and summer in the storm recovery phase.

But, if a magnetic storm commences in the afternoon/evening sector, foF2 falls first in the main phase and then in the recovery phase. Sometimes foF2 falls in the initial storm phase indicated by the increase of the AE and Kp indices. If the magnetic storm commences in the morning or night hours, foF2 falls only in the recovery phase, which can persist for a long time.

Table 2
List of storms with the observed fall of the foF2.

Date	Dst_{min}	UT_{min}	*N*	Phase of storm
06–08. 04. 2000	−320	01 (m)	1	Recovery
17–20. 09. 2000	−200	23 (m)	1	Recovery
17–21. 04. 2002	−125, −150	13 (e)	4	Initial, main, recovery, recovery
01–06. 10. 2002	−158, −146	13 (e)	3	Main, recovery, recovery
13–16. 10. 2003	−52, −85	12 (e)	1	Main, recovery
22–24. 10. 2003	−49, −60	01 (m)	2	Recovery, recovery
9–14. 03. 2004	−71, −63	20 (n)	3	Recovery, recovery, recovery
03–07. 04. 2004	−112, −80	01 (m)	3	Initial, recovery, recovery
12–16. 10. 2004	−57	06 (a–n)	2	Main, recovery
07–10. 05. 2005	−89, −127	07 (a–n)	2	Main, recovery
15–19. 05. 2005	−263	09 (e)	3	Recovery, recovery, recovery
23–26. 08. 2005	−243	12 (e)	3	Initial, main, recovery
31.08–04.09. 2005	−134	21 (m)	4	Initial, recovery, recovery, recovery
04–06.04.2006	−87	07 (a–n)	2	Main, recovery
13–16.04.2006	−111	10 (e)	2	Main, recovery
19–22.08.2006	−73	21 (m)	2	Recovery, recovery
23–25.09.2006	−55	09 (a–n)	2	Main, recovery
23–26.03.2007	−71	08 (a–n)	2	Initial, main

The data, Dst_{min}, UT of the Dst_{min} or the first Dst_{min} if the storm has not only minimum, the number of the events of the fall of the foF2 and the storm phase are presented. The letters in the brackets mean the time of day in LT: m—morning; e—evening; n—night and a–n—afternoon.

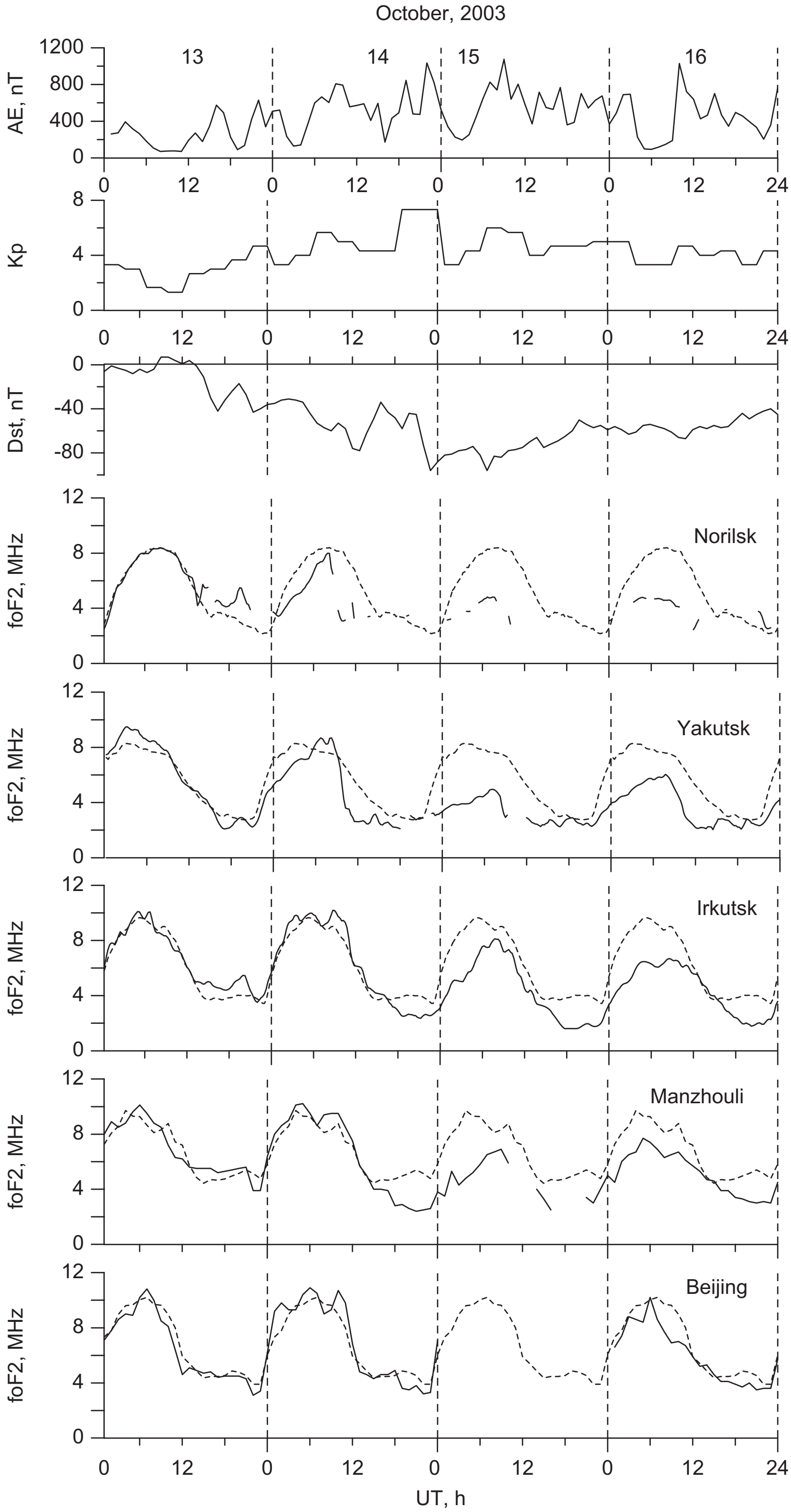

Fig. 1. Variations in F2-layer critical frequencies during the magnetic storm on 13–16 October 2003. Dashed lines show the undisturbed day, solid lines correspond to the current foF2 values. The AE, Kp and Dst values are shown on the top of the figure. LT = UT+Δt, where Δt equals to 6–8 h depending on the longitude of a station (see Table 1). The foF2 fall was observed at subauroral stations in the evening hours on October 14–16.

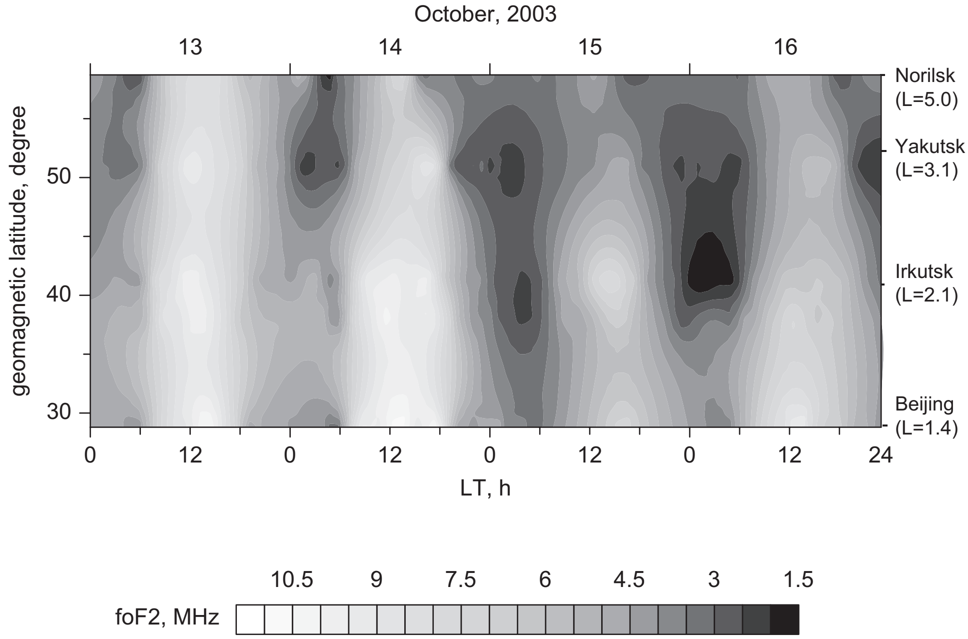

Fig. 2. Maps of the foF2 isolines in the LT–geomagnetic latitude coordinate system for the magnetic storm on 13–16 October 2003. At the quite night on 13–14 October, MIT was located in the magnetic latitudes over 50°. The narrow trough appeared at ~19 LT and widens rapidly to the north and south and attains a width of ~6° at midnight. Then the equatorward MIT wall moved fast to the low latitudes (~35°). The polar wall location changed insignificantly. The MIT width reached 20°. Next night on 15–16 October, the polar wall held its position, whereas the equatorward wall was coming back very slowly.

Analysis of the vertical sounding data and geomagnetic indices reveals that afternoon troughs can be observed in the subauroral latitudes ($L>3$) during substorms, when $250<\mathrm{AE}<1000$ nT and $\mathrm{Kp}>3$. They are associated with the MIT motion to the middle latitudes. During the main storm phase, there are no F2-layer reflections at high-latitude ionograms, because of both absorption and blanketing by Es layers.

Fig. 1 presents foF2 variations at the chain of stations during the moderate storm on 13–16 October 2003. The hourly foF2 values averaged over several quiet days of the month are used as the quiet level.

Obviously, the fall of the foF2, designed by Whalen (1987, 1989) as "bite-out", was seen in the subauroral latitudes (Norilsk and Yakutsk) during the magnetic storm main phase in the evening, when $\mathrm{Dst}=-60$ nT. The index AE increased to 1000 nT at the same time. Before the foF2 fall, the anomalous ionization-density increase (by ~1 MHz) was recorded at all stations except at Norilsk. In the middle latitudes, the density decreased considerable at night, and the foF2 was less than 2 MHz from Norilsk to Manzhouli. In the daytime, the density was very low, especially at high latitudes (ΔfoF2 is about 50%). In the recovery phase, the density dropped on the background of the low ionization in Norilsk and Yakutsk in the evening on 15 and 16 October. The night density in the F region remained very low.

Fig. 2 presents the foF2 variations in the LT–geomagnetic latitude coordinate for this period. The map of the foF2 isolines shows that the MIT region ($\mathrm{foF2}<3$ MHz) was located in the geomagnetic latitudes 47–55° at 01–05 LT on 13 and 14 October. The foF2 isolines became distorted in the evening on 14 October. The drop of density occurred in Norilsk at 16 LT and moved to the lower latitude. The low-ionization region expanded equatorward up to the geomagnetic latitude 35° from 22 LT on 14 October to 06 LT on 15 October. The polar MIT wall was in the latitude ~55°. The equatorward wall moved slowly back next night. The MIT ranged in width 20–25°.

A similar situation was observed in data from the satellite "Intercosmos-19" (Indyukov et al., 1985). As deduced from the topside sounding, the polar wall motion agreed well with the Kp index. But the location of the equatorward wall after the storm differed from that before the storm. After the storm, the very low electron density extended to the geographic latitudes 30–35°. Then the equatorward wall came back for 4–6 days.

The variations of the total electron content during the magnetic storm showed that the equatorward boundary of low night values remained in the geographic latitude ~40° for several days after the storm (Afraimovich et al., 2002).

The foF2 variations during the magnetic storm with the minimum of $\mathrm{Dst}=-130$ nT are presented in Fig. 3. The foF2 started falling during the initial storm phase in Zhigansk and Yakutsk on 31 August. The anomalous ionization in the F and E layers associated with the polar wall of the MIT was observed in Norilsk. The F2-layer reflections were absent during the main phase, which coincided with the local night. The analysis of the ionograms revealed that the blanketing Es layers with the frequencies of 6–7 MHz were observed in that period. The intensive negative disturbances (to 50%) occurred in

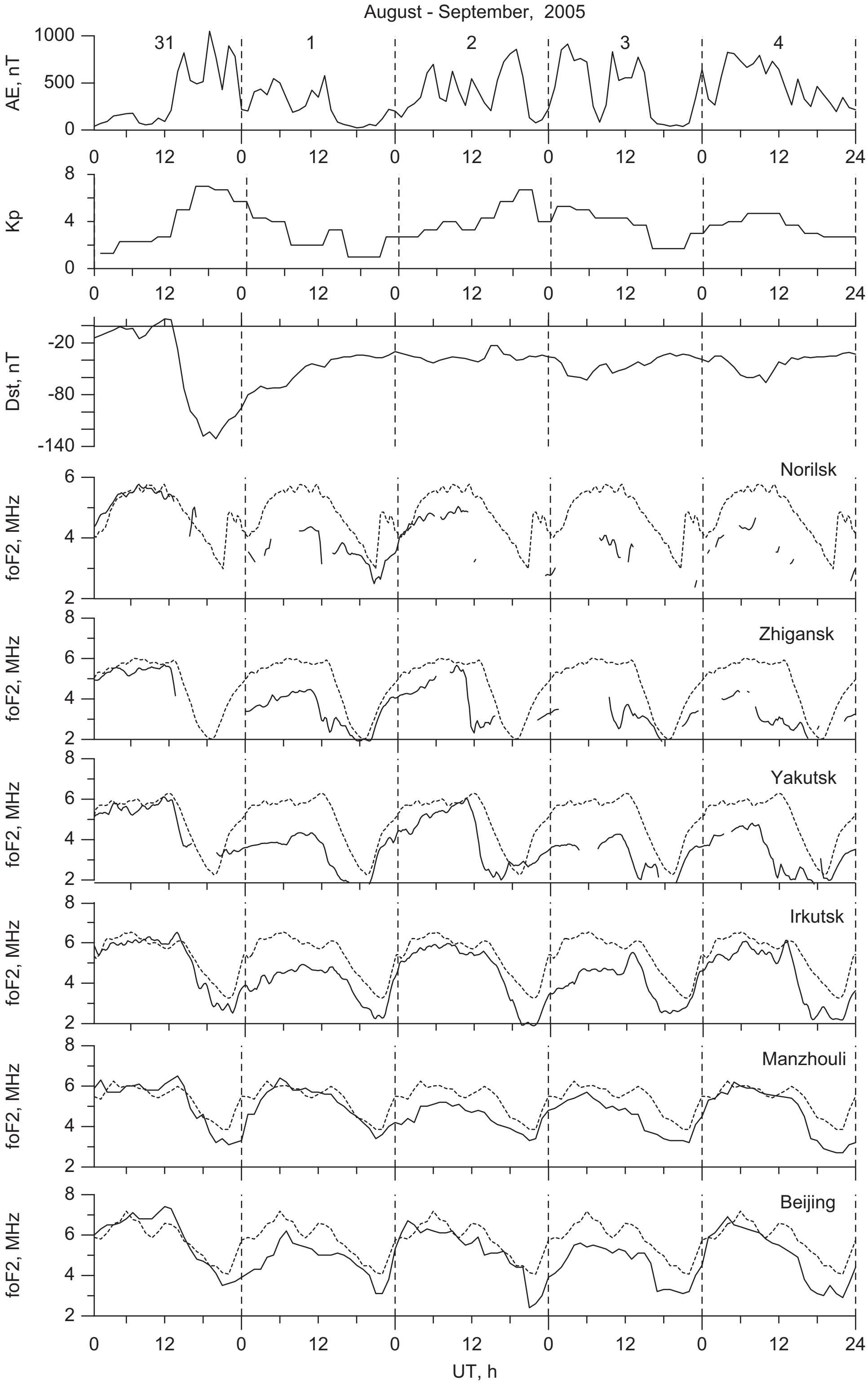

Fig. 3. Variations of foF2 on 31 August–04 September 2005. The foF2 falls were observed every evening in both initial and recovery phases of the magnetic storm.

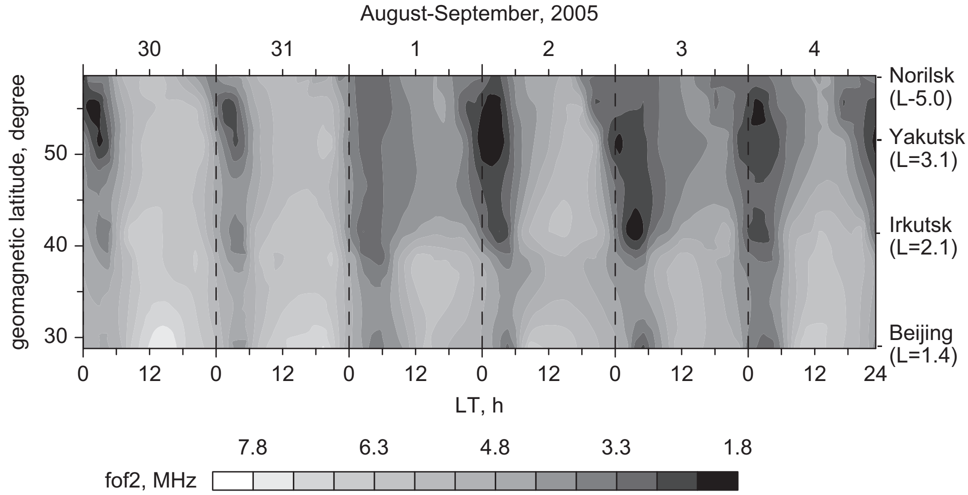

Fig. 4. Maps of the foF2 isolines in the LT–geomagnetic latitude coordinate system on 30 August–04 September 2005. The MIT region (foF2 < 3 MHz) was located in the geomagnetic latitudes 50–55° at 01–04 LT in the quite days on 30 and 31 August. After midnight on 1 September, the MIT combined with the region of low ionization, caused by the storm, and expanded to the equator to the geomagnetic latitude 35°. The daytime density was very low. The MIT equatorward wall was in the high latitudes at ~18 LT on 1 August and moved to the low latitudes after midnight on 2 August. The MIT polar wall was in the latitude >55°. The MIT width was ~20–25°. Only on 4 August, both the equatorward and polar walls of the MIT returned.

the daytime during the recovery phase on September 1. The evening fall of foF2 developed on the background of the low ionization in Norilsk and Zhigansk. The foF2 values began to recover to their quiet level on 2 September, but the increase of Kp and AE indices produced a new fall of foF2. On 3 and 4 September, the evening trough formed on the background of the low ionization at the subauroral stations. Note that the night foF2 values were low at all stations of the chain. On 3 September, the foF2 increased to 3–4 MHz in the high latitudes, because of auroral fluxes at the polar MIT wall. This is associated with a sharp increase of AE.

Fig. 4 implies that the MIT region (foF2 < 3 MHz) was situated in the geomagnetic latitudes 50–55° at 01–04 LT during the quiet days of 30 and 31 August. But after midnight (on 1 September) at the Dst minimum, the MIT combined with the region of the low ionization, caused by the storm, and expanded equator to the geomagnetic latitude 35° from 00 to 06 LT. The daytime density is always very low. The equatorward MIT wall was observed in the high latitudes at ~18 LT on 1 August; it was moving to the low latitudes on 2 August after midnight. The polar MIT wall was in the latitude >55°. On 3 August after midnight, the equatorward wall held its position, while the polar wall was moving to the geomagnetic latitude ~53°. On 4 August, both the equatorward and polar walls of the MIT came back. The MIT width was ~20–25°.

The above examples of the afternoon/evening troughs illustrate that such troughs arise in the main phase of a magnetic storm, if the storm commences in the afternoon/evening sector. Otherwise, the afternoon/evening trough can be observed in the recovery phase. The region of the anomalously low night ionization (MIT) expands to the middle latitudes and its equatorward wall is coming back over several days after the storm. The MIT ranges in width 20–25°. The MIT structure is fixed in the local time.

3. Modeling

Some preliminary model calculations of electron density variations during the observation of afternoon/evening troughs were carried out, and the contribution of different processes to the trough formation was estimated. We applied the theoretical ionospheric model developed at the Institute of Solar-Terrestrial Physics, Russian Academy of Sciences, Irkutsk, Russia (Tashchilin and Romanova, 2002). This model is based on a numerical solution of the system of nonstationary equations of the balance of particles and thermal plasma energy within closed geomagnetic-field tubes, whose bases are at a height of 120 km.

Plasma is assumed to consist of atomic O^+, H^+, N^+, He^+, molecular N_2^+, O_2^+, and NO^+ ions. We calculated the densities of all ions, except for N_2^+, taking into account the processes of photoionization, impact ionization by the magnetospheric electrons, recombination, transport along geomagnetic-field lines due to the ambipolar diffusion, and ion drag by the horizontal thermospheric wind. The plasma drift across magnetic field lines was also considered. The reference spectrum of the EUV radiation from Richards et al. (1994) was used to calculate the photoionization of thermospheric constituents and energy spectra of primary photoelectrons.

We calculated electron and ion temperatures, taking into account the heat conduction processes along geomagnetic-field lines and the thermal energy exchange between electrons, ions, and neutral species due to elastic and inelastic collisions. The rate of the thermal electron heating was calculated self-consistently by solving the kinetic equation of the photoelectron transport in the conjugated ionospheres.

The global empirical thermospheric model MSIS-86 was used to describe space–time variations in temperature and concentration of neutral constituents. Velocities of the horizontal thermospheric wind were determined from the HWM-90 model (Hedin et al., 1991).

The values of the integral flux and mean energy of precipitating electrons necessary to calculate the auroral ionization rates were taken from the global model of electron precipitation by Hardy et al. (1987). The magnetospheric convection electric field was determined with the empirical model of potential distribution (Sojka et al., 1986).

We reproduced the ionosphere response to the magnetic storms under study by calculating variations of plasma parameters within the entire magnetic field tube, whose basis was located in the Northern hemisphere at the points with the geographical coordinates of the ionospheric stations shown in Table 1.

To obtain spatial distribution of the charged particle density and temperatures at a certain time UT, it is necessary to simultaneously integrate the system of model equations for a set of plasma tubes that move along different drift trajectories. Thus the general solution algorithm is divided into two stages. At the first stage, a drift trajectory is calculated by integrating the equations of plasma tube motion under the action of convection electric fields and corotation backward in time from a given UT to a certain initial time UT_0. Time variations of the electric field are considered through the use of actual hourly values of variations of the geomagnetic activity indexes (Kp, Ap) and IMF components (Bz, By) (the input parameters for the empiric model of the electric field).

At the second stage, we calculate initial profiles of ion densities and temperatures along field lines. Then the equations of ionospheric plasma balance are integrated forward along the drift trajectories from UT_0 to a given UT. Variations in parameters of precipitations, neutral atmosphere, and thermospheric wind are also taken into account due to actual variations in the hourly geomagnetic activity indices.

The moderate storm with two minima in April 2004 was chosen for modeling. Fig. 5 shows foF2 variations at one mid-latitudinal and three subauroral stations. The first Dst minimum coincided with the morning in LT. Thus, large negative disturbances were observed in the daytime on 4 April. The foF2 fall occurred on 5 April and was most pronounced on 6 April in the storm recovery phase.

It is very important to define the input parameters such as the electric field of the magnetospheric convection, auroral fluxes of energetic particles, and parameters of the neutral atmosphere to model the ionosphere response to a magnetic storm.

As is known, the model MSIS-86 does not allow the correct reproduction of parameters of the thermosphere during disturbances. The GUVI data were used to correct the MSIS-86 (http://guvi.jhuapl.edu/guvi_accessdata.html).

The correction coefficients were calculated as follows:

$$k_{GUVI} = \frac{R_{GUVI}}{R^0_{GUVI}}, \quad k_{MSIS} = \frac{R_{MSIS}}{R^0_{MSIS}} \qquad \text{where } R = \frac{[O]}{[N_2]},$$

R_{GUVI} is the GUVI data, R_{MSIS} the one calculated by MSIS, R^0_{GUVI}, R^0_{MISS} the corresponding rations on a quiet day. A corrective factor is determined as k_{GUVI}/k_{MISS}.

The GUVI data on 2 April 2004 were used to calculate R^0_{GUVI}. For example, at 02 UT on 6 April 2004 $k_{GUVI} = 2$, $k_{MISS} = 1.78$; thus, the corrective factor is equal to 1.23. The modeling results obtained with this correction are denoted as Variant 1.

The empirical models of auroral precipitation and the electric field of the magnetospheric convection used in the calculations need a correction for the magnetic storm. For this purpose, we used the DMSP data (http://sd-www.jhuapl.edu/Aurora/ovation/ovation_display.html). Fig. 6(b, d) presents the electron energy fluxes calculated from the model by Hardy et al. (1987) and the auroral oval equatorial and polar boundaries from the DMSP data (thick lines) in the quiet day on 2 April and during the storm on 6 April 2004.

Fig. 6(d) shows that the auroral oval equatorial boundary obtained from the DMSP data was located 5–7° lower than that from the empirical model.

The magnetospheric convection electric potential calculated from the model by Sojka et al. (1986) is presented in Fig. 6(a, c). According to Sojka et al. (1986), the morning–evening potential drop during a disturbance is 70–90 kV, whereas it is known that this magnitude can be 100–150 kV (Chappel, 1988).

In order to correct the empirical model (Sojka et al., 1986), the formula of the potential drop across the polar cap $\Delta\phi_{PC} = 10+6.5$ Kp is changed to $\Delta\phi_{PC} = 10.06+14.4$ Kp, obtained from the Millstone Hill Incoherent Scattering Radar (ISR) data (Oliver et al., 1983). The convection equatorial boundary was extended southward by 10°. The correctness of such changes was discussed by Fuller-Rower et al. (1994). The electric potential calculated with these corrections is presented in Fig. 6(e). The modeling results obtained in such a way are denoted as Variant 2.

Fig. 5 presents the calculation results obtained by Variant 1 (the thin solid curves). Circles denote foF2 measurements and dashed curves indicate the foF2 values for the quiet day. A good agreement between the measured and calculated foF2 values obtained during the quiet and moderately disturbed periods. The fall foF2 is not displayed by the thermospheric composition correction only. As stated above, this can be caused by MIT displacement and expansion. To reproduce the MIT appearance above stations Norilsk, Zhigansk, and Yakutsk, the modeling results were obtained with Variant 2. Fig. 5 (the thick solid line) shows that the foF2 fall is reproduced at all said stations in this variant. The exception is the difference between calculations and measurements of foF2 at the mid-latitudinal station Irkutsk in the evening and nighttime. Similar phenomenon has extensively been studied in Romanova et al. (2006).

To analyze the obtained results, we calculated the global distribution of electron density and electromagnetic drift velocities with regard to the corotation for the quiet day of 2 April 2004 and the disturbed day of 6 April 2004 at 10, 12, and 14 UT. Fig. 7 shows variations of the lgNe values at a height of 300 km in the geomagnetic latitude—the MLT coordinate system for Variants 1 and 2. The calculated velocities of the electromagnetic drift with corotation W are indicated by arrows. The eastward electromagnetic drift (anti-clockwise in the figure) with

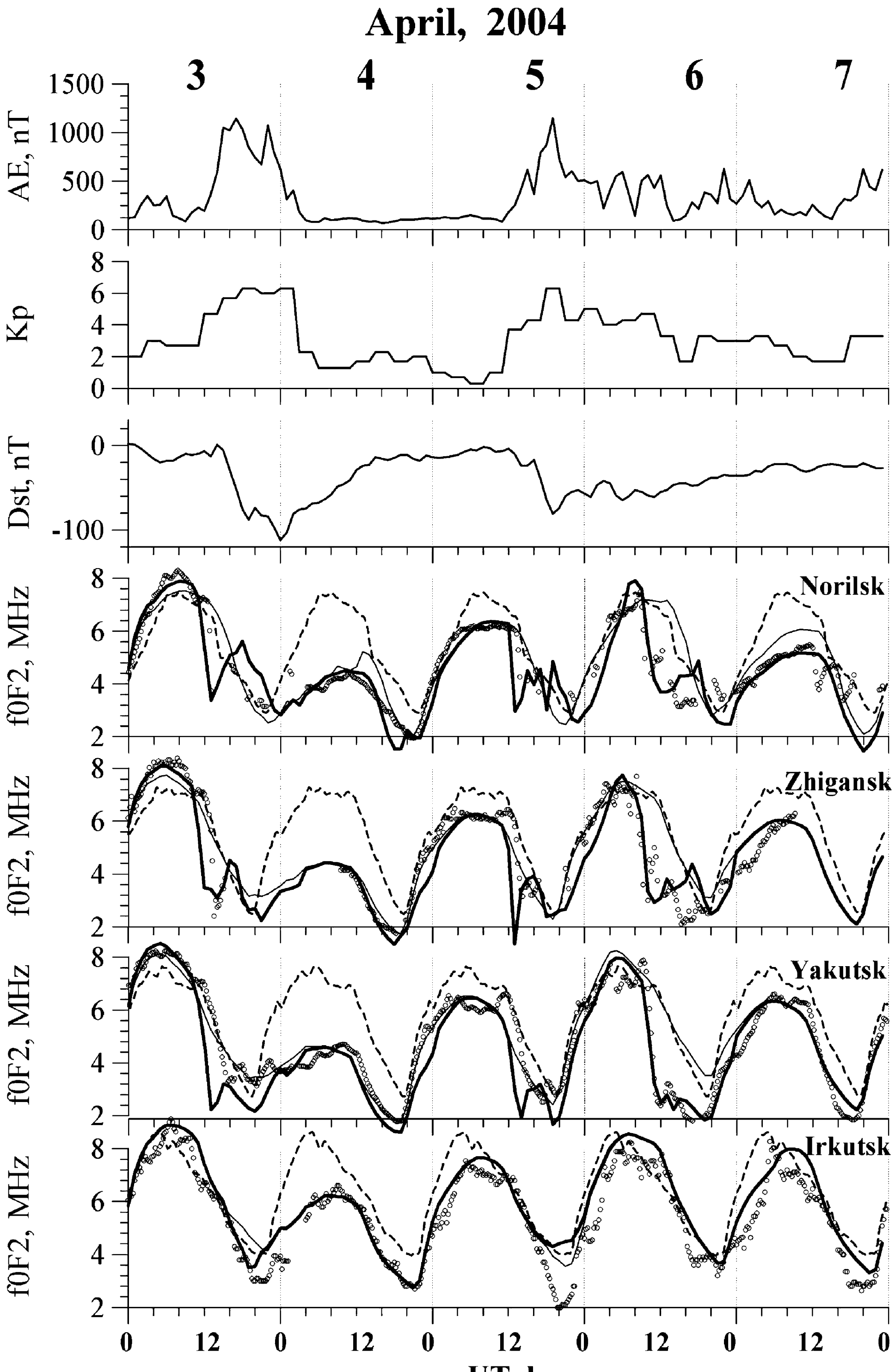

Fig. 5. Variations of observed and calculated foF2 at the chain of four stations on 3–7 April 2004. The AE, Kp, and Dst values are presented on the top. Circles indicate the foF2 measurements; dashed curves show the quiet level. Thin solid curves present the foF2 calculated with Variant 1. Thick solid curves correspond to the calculations by Variant 2.

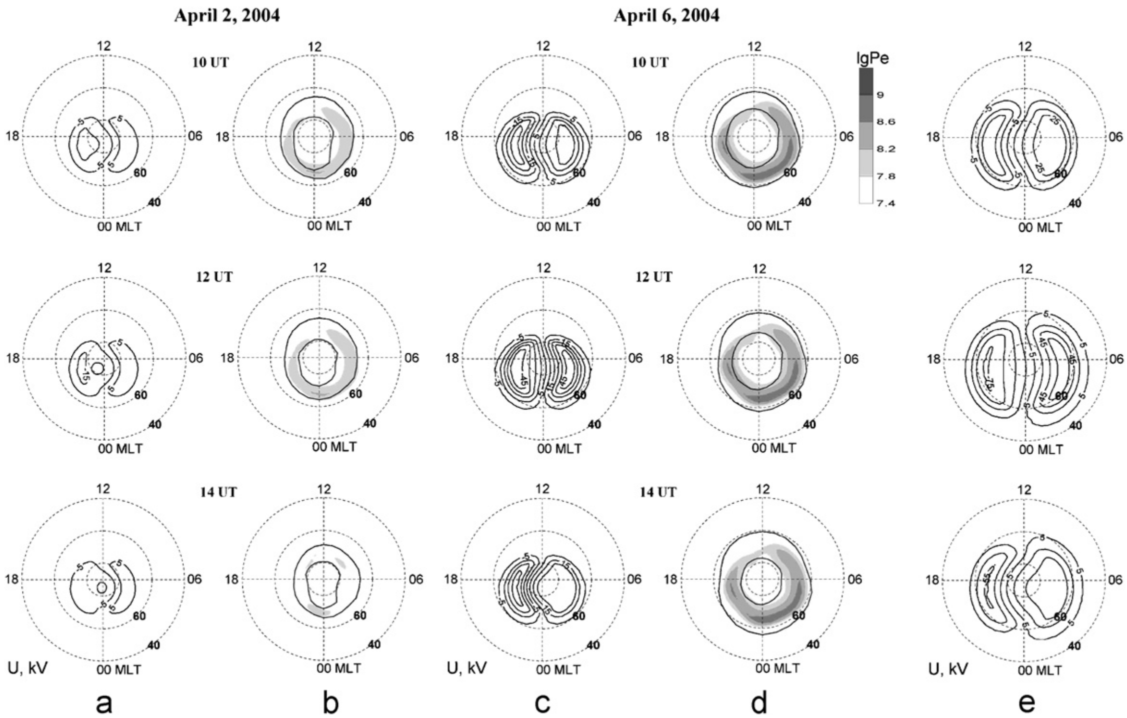

Fig. 6. The electric potential of the magnetospheric convection calculated from the empirical model of potential distribution (Sojka et al., 1986) without a correction (a,c) and with it (e). Panels (b) and (d) are the logarithms of the precipitating electron energy flux calculated from the model by Hardy et al. (1987); the thick lines are the equatorial and polar boundaries of auroral oval from the data DMSP.

the velocity of ~200 m/s prevails in the quiet day. There were some minor deviations in the polar cap. MIT formed in the nighttime sector owing to the slow plasma drift in the absence of ionization sources. The drift led to the recombination of plasma to very low values. Differences in the MIT location and form at different UT hours can result from UT variations (Tashchilin and Romanova, 2002). According to the results of the modeling of the 6 April storm by Variant 1 (Fig. 7b), the MIT was in the sector from 22 to 04 MLT at 10 UT. All stations were exterior to the trough, while our observations testify that the MIT was most likely to be over the stations at that time. According to the results of the modeling with Variant 2 (Fig. 7c), MIT was narrow and situated between 17 and ~07 MLT at 10 UT. Obviously, the trough in the evening time resulted from transport of the low-density plasma by the westward drift from the nighttime side to the evening sector. The drift velocity ran up to ~700 m/s from 13 to 20 MLT in the geomagnetic latitudes 55–65°. The MIT location also coincided with the eastward drift with high velocities of ~1000–1200 m/s from 00 MLT to 07 MLT. The drift transported the low-density plasma from the nighttime to the morning sector, resulting in the trough on the morning side. At 12 and 14 UT, a belt of eastward drift was also formed on the nighttime side (velocities were ~1000–1300 m/s), which coincided with the MIT location. The MIT location in the afternoon sector agreed with the belt of the westward drift (~700 m/s) that existed from 13 to 21 MLT within the geomagnetic latitudes 55–65°.

4. Discussion

The preceding sections describe some important properties of the afternoon/evening trough.

This study reveals that the fall of foF2 in the afternoon/evening sector in East Asia can mainly be observed in equinox or between equinox and summer. This result is inconsistent with the definition of the afternoon/evening trough as a winter event. The point is that the preceding investigations used data obtained during winter periods (Whalen, 1987; Besprozvannaya et al., 1986).

If a magnetic storm commences in afternoon and evening hours, the density firstly drops in the main phase, then in the recovery phase. Sometimes this occurs before a storm indicated by AE and Kp increases. If a magnetic storm starts in morning or night hours, foF2 falls only in the recovery phase.

After the density drops, the low-ionization region extends to middle latitudes, forming a wide trough.

The foF2 fall correlates with the indices AE and Kp better than with Dst.

The foF2 fall in the afternoon/evening sector can be explained by the westward plasma convection at high velocities caused by intense electric fields. Satellite measurements show that during geomagnetic storms the intense poleward electric fields (~250 mV/m) can be observed on the equatorial wall of the auroral zone (Rich et al., 1980). These fields are responsible for westward drifts with high velocities. According to observations with the ISR, the velocities are over 1000 m/s

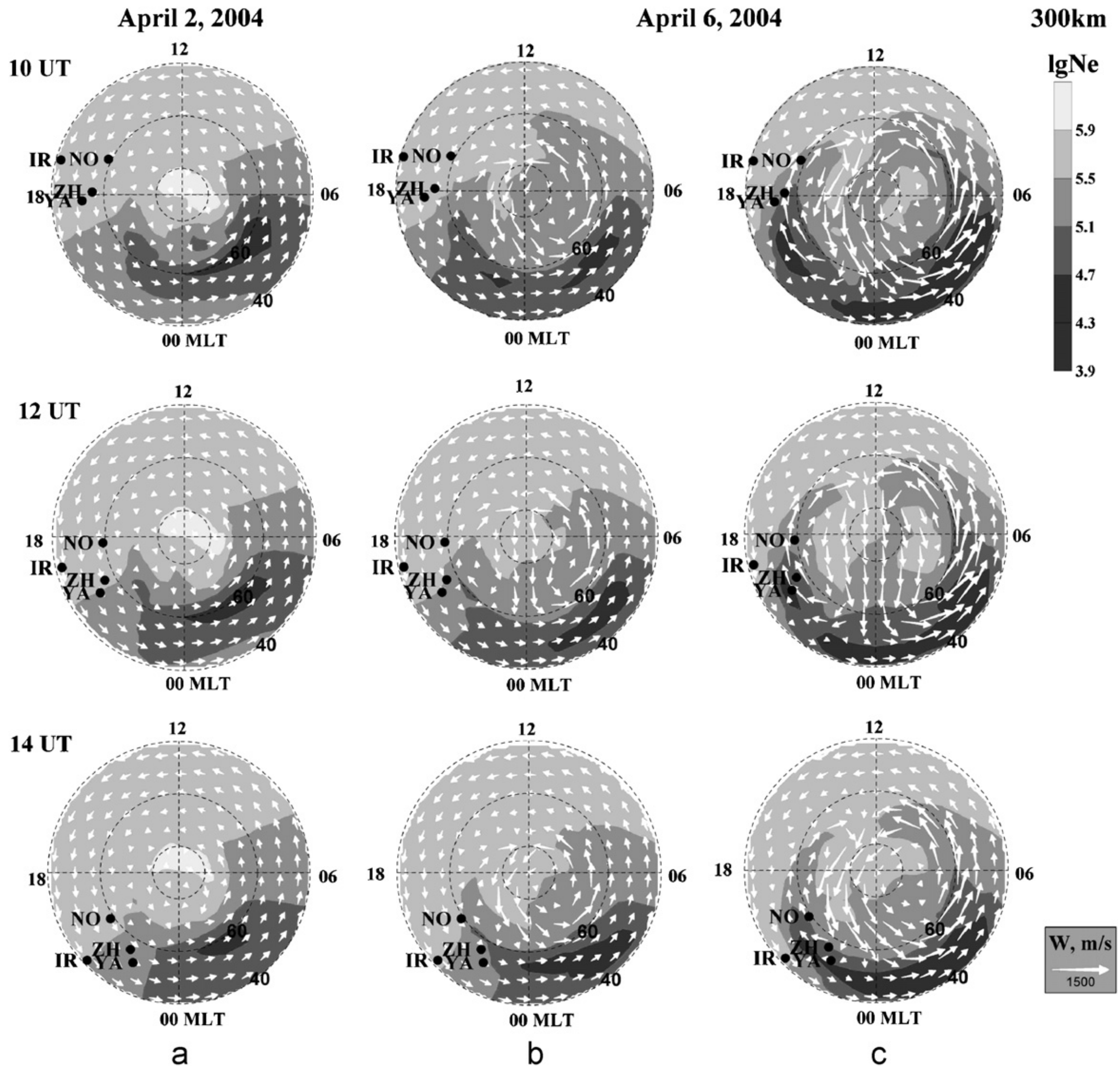

Fig. 7. Variations of lgNe values at a height of 300 km in the geomagnetic latitude—the MLT coordinate system for Variants 1 (a,b) and 2 (c). Calculated velocities of the electromagnetic drift with corotation *W* are shown by arrows, dots indicate locations of the station.

(Holt et al., 1984; Foster, 1993). The high velocities lead to deepening of a trough and its expansion to the day sector. SAID are associated with disturbed conditions, and specifically with the substorm recovery phase (Anderson et al., 1993). The result of the simultaneous satellite and ground-based measurements of the fast SAID effects show that the development of a narrow belt of a westward drift with high velocities (polarization jet) causes the intensive depletion of electron density in the F2 layer for 15–20 min (Khalipov et al., 1977; Galperin et al., 1986). This is consistent with the fast formation or deepening of the trough in the background ionization.

Model calculations of electron density variations during the evening ionization gradients, presented in this study, support the assumption that the narrow and deep trough in the afternoon sector is formed by the westward drift with high velocities.

Simultaneous measurements of electron density, ion and electron temperatures and ion drift by the ISR detect the high values of Ti and Te and drift velocity in the ionospheric trough (Holt et al., 1984; Lockwood et al., 1984). This permits us to suppose effects of enhanced recombination. In this case the trough with the abrupt equatorial wall appears and extends to the day sector.

Thus an explanation for abrupt decreases of F2-layer critical frequencies in afternoon/evening hours can be the effect of plasma fast convection in a westward direction caused by intense electric fields. The disturbed variations of neutral winds, composition changes, and enhanced recombination can also produce the observed effects.

5. Conclusion

The presented investigations of the MIT appearance in the afternoon/evening sector in East Asia allow the following conclusions.

The foF2 fall in the afternoon/evening is associated with the formation of the deep equatorial wall of the MIT during magnetic substorms.

The afternoon/evening ionospheric trough is observed in the subauroral latitudes of East Asia predominantly in equinox or between equinox and summer. If a magnetic storm commences in the afternoon/evening sector, foF2 falls firstly in the main phase and then in the recovery phase. If a magnetic storm begins in morning or night hours, foF2 falls only in the recovery phase.

The low-ionization region (MIT) expands to the middle latitudes. The MIT ranges in width from 20° to 25°. Its equatorward boundary is coming back over several days upon completion of a magnetic storm.

The model results show that MIT in the afternoon sector is formed by the westward drift that transports the low-density plasma from the night side with velocities $\sim$700 m/s. The east drift with high velocities ($\sim$1000–1200 m/s) transports the low-density plasma from the night to morning sides, resulting in a trough on the morning side.

Acknowledgment

This work was supported by the Russian Foundation for Basic Research (Grants 07-05-00950-a and 07-05-92100).

References

Afonin, V.V., Benkova, N.P., Besprozvannaya, A.S., Shchuka, T.I., Zikrach, E.K., Shestakova, L.V., 1995. The ionospheric trough dynamics in the northern and southern hemispheres: the longitudinal and IMF effects. Journal of Atmospheric and Terrestrial Physics 57, 1057–1062.

Afraimovich, E.L., Kosogorov, E.A., Leonovich, L.A., Palamarchouk, K.S., Pirog, O.M., 2002. Global pattern of large-scale ionospheric disturbances during the magnetic storm of September 25, 1998, as inferred from GPS network data. Geomagnetizm and Aeronomy 42, 1–8.

Afraimovich, E.L., Lesyuta, O.S., Perevalova, N.P., Pirog, O.M., Smirnov, V.F., Zikrach, E.k., Bondar, E.D., 2005. Study of the main ionospheric trough based on the data of the GPS and ionospheric stations in the Yakutsk region. Geomagnetizm and Aeronomy 45, 203–208.

Anderson, P.C., Hanson, W.B., Heelis, R.A., Craven, J.D., Baker, D.N., Frank, L.A., 1993. A proposed production model of rapid subauroral ion drifts and their relationship to substorm evolution. Journal of Geophysical Research 98, 6069–6078.

Benkova, N.P., Kozlov, Ye.F., Mozhayev, A.M., Osipov, N.K., Samorokin, N.I., 1980. Main ionospheric trough in the daytime sector, according to vertical sounding data. Geomagnetizm and Aeronomy 20, 817–821.

Besprozvannaya, A.S., Pirog, O.M., Shchuka, T.I., 1986. Latitudinal-temporal peculiarities of the postnoon ionization of the F2 layer according to data of a meridional chain of ionospheric stations. Geomagnetizm and Aeronomy 20, 320–322.

Buonsanto, M.J., 1999. Ionospheric storms—a review. Space Science Review 88, 563–601.

Chappel, C.R., 1988. The terrestrial plasma source: a new perspective in solar-terrestrial processes from Dynamics Explorer. Research of Geophysics 26, 229–237.

Collis, P.N., Haggstrom, I., 1988. Plasma convection and auroral precipitation processes associated with the main ionospheric trough at high latitudes. Journal of Atmospheric and Solar-Terrestrial Physics 50, 389–404.

Deminov, M.G., Karpachev, A.T., 1986a. Longitudinal effects in the configuration of the main ionospheric trough. I. Position of the trough. Geomagnetizm and Aeronomy 26, 48–52.

Deminov, M.G., Karpachev, A.T., 1986b. Longitudinal effects in the configuration of the main ionospheric trough. II. Shape of the trough. Geomagnetizm and Aeronomy 26, 574–585.

Evans, I.V., Holt, J.M., Oliver, W.L., Wand, R.H., 1983a. The "fossil" theory of nighttime high latitude F-region troughs. Journal of Geophysical Research 88, 7769–7782.

Evans, J.V., Holt, J.M., Wand, R.H., 1983b. On the formation of daytime troughs in the F-region within the plasmasphere. Geophysical Research Letters 10, 405–408.

Foster, J.C., 1993. Storm-time plasma transport at middle and high latitudes. Journal of Geophysical Research 98, 1675–1689.

Fuller-Rower, T.J., Codrescu, M.V., Moffett, R.J., Quegan, S., 1994. Response of the thermosphere and ionosphere to geomagnetic storms. Journal of Geophysical Research 99, 3893–4011.

Galperin, Y.I., Khalipov, V.I., Filipov, V.M., 1986. Signature of rapid subauroral ion drifts in high-latitude ionosphere structure. Annals of Geophysics 4, 145–154.

Hardy, D.A., Gussenhoven, M.S., Raistrick, R., 1987. Statistical and functional representation of the pattern of auroral energy flux, number flux, and conductivity. Journal of Geophysical Research 92, 12275–122294.

Hedin, A.E., Biondi, M.A., Burnside, R.G., et al., 1991. Revised global model of thermosphere winds using satellite and ground-based observations. Journal of Geophysical Research 96, 7657–7688.

Holt, J.M., Wand, R.H., Evans, J.V., 1984. Millstone Hill measurements 26.02.79 during the solar eclipse and formation of a midday F-region trough. Journal of Atmospheric and Solar-Terrestrial Physics 46, 251–254.

Indyukov, A.E., Klimov, N.N., Vasilyev, G.V., Fligel, M.D., 1985. On the location of the main ionospheric trough from topside sonding data. Issledovaniya of Geomagnetizm, Aeronomii and Physics Solntsa 71, 49–53.

Khalipov, V.I., Galperin, Y.I., Lisakov, Yu.V., Filipov, V.M., 1977. Diffuse auroral zone II. Cosmic Research 17, 708–733.

Kurkin, V.I., Matyshonok, S.M., Pirog, O.M., Poddelsky, I.N., Ponomarchuk, S.N., Rosanov, S.V., Smirnov, V.F., 2006. The dynamics of the auroral oval and ionospheric trough boundaries according to data from the DMS satellites and ground-based ionosonde network. Advances in Space Research 38, 1772–1777.

Lockwood, M., 1980. The bottomside mid-latitude ionospheric trough. Journal of Atmospheric and Solar-Terrestrial Physics 42, 605–615.

Lockwood, M., Farmer, A.D., Opgencorth, H.J., 1984. EISCAT observations of plasma convection and the high-latitude winter F-region during substorm activity. Journal of Atmospheric and Solar-Terrestrial Physics 46, 489–499.

Oliver, W.L., Holt, J.M., Wand, R.H., 1983. Millston Hill incoherent scatter observations of auroral convection over $60^\circ < \Lambda < 75^\circ$. 3. Average patterns versus Kp. Journal of Geophysical Research 88, 5505–5524.

Prölss, G.W., 2007. The equatorward wall of the subauroral trough in the afternoon/evening sector. Annals of Geophysics 25, 645–659.

Prölss, G.W., Brace, L.H., Mayer, H.G., et al., 1991. Ionospheric storm effects at subauroral latitudes: a case study. Journal of Geophysical Research 96, 1275–1288.

Rich, F.J., Burke, W.J., Kelly, M.C., Smiddy, M., 1980. Observations of field-aligned currents in association with strong convection electric field at subauroral latitudes. Journal of Geophysical Research 85, 2335–2342.

Richards, P.G., Fennelly, J.A., Torr, D.G., 1994. EUVAC: A solar EUV flux model for aeronomic calculations. Journal of Geophysical Research 99, 8981–8992.

Rodger, A.S., Moffett, R.J., Quegan, S., 1992. The role of ion drift in formation of ionisation troughs in the mid- and high-latitude ionosphere—a review. Journal of Atmospheric and Solar-Terrestrial Physics 54, 1–30.

Romanova, E.B., Tashchilin, A.V., Zherebtsov, G.A., Pirog, O.M., Polekh, N.M., Smirnov, V.F., Stepanov, A.E., Shi, J.K., Wang, X., 2006. Modeling of the seasonal effects of geomagnetic storms in the Eastern Asia ionosphere. International Journal of Geomagnetism and Aeronomy 6, GI3003.

Sojka, J.J., Rasmussen, C.E., Schunk, R.W., 1986. An interplanetary magnetic field dependent model of the ionospheric convection electric field. Journal of Geophysical Research 91, 11281–11290.

Tashchilin, A.V., Romanova, E.B., 2002. Numerical modeling the high-latitude ionosphere. Proceedings of COSPAR Colloquia Series 14, 315–325.

Tsunoda, R.T., 1988. High-latitude F region irregularities: a review and synthesis. Reviews of Geophysics 26, 160–719.

Vo, H.B., Foster, J.C., 2001. A quantitative study of ionospheric density gradients at midlatitudes. Journal of Geophysical Research 106, 21555–21563.
Whalen, J.A., 1987. Daytime F-layer trough observed on a macroscopic scale. Journal of Geophysical Research 92, 2571–2576.
Whalen, J.A., 1989. The daytime F layer trough and its relation to ionospheric-magnetospheric convection. Journal of Geophysical Research 94, 17169–17184.
Zherebtsov, G.A., Pirog, O.M., Razuvaev, O.I., Besprozvannaya, A.S., Shchuka, T.I., 1993. The dynamics of the polar edge of the trough deduced using data from a meridional chain of vertical-incidence sounding stations. Journal of Atmospheric and Solar-Terrestrial Physics 55, 1537–1542.